Proceedings of the 2017 Winter Simulation Conference
W. K. V. Chan, A. D'Ambrogio, G. Zacharewicz, N. Mustafee, G. Wainer, and E. Page, eds.

DESIGN METHODOLOGY TO SIMULATE CONTINUOUS DESCENT OPERATIONS AT KANSAI INTERNATIONAL AIRPORT

Daichi Toratani
Navinda Kithmal Wickramasinghe
Sachiko Fukushima
Hiroko Hirabayashi

Air Traffic Management Department
Electronic Navigation Research Institute (ENRI)
7-42-23 Jindaijihigashimachi
Chofu, Tokyo 182-0012, JAPAN

ABSTRACT

One of the hot topics in the field of air traffic management is continuous descent operations, which is one of the efficient descent procedure to an airport. In Japan, the continuous descent operations are implemented at Kansai International Airport, but its applicability is limited to only the non-congestion period owing to the unpredictability of the trajectory and arrival time of the continuous descent operations as compared to the conventional operations. To expand the time period for the continuous descent operations, in this paper, we develop a fast-time simulator. The simulator can provide the predicted trajectory and arrival time of the continuous descent operations. The prediction accuracy is reviewed by comparison with the results of the simulation conducted on a full flight simulator. Discussions on accuracy improvement of the prediction have been provided considering available data for air traffic controllers through radar data systems.

1 INTRODUCTION

Continuous descent operations (CDO) has been considered key solutions for reducing fuel consumption and as noise abatement procedures (Clarke et al. 2004). In Japan, the CDO has been implemented at Kansai International Airport (KIX) (Kansai Airports 2016). However, its applicability is limited to only the non-congestion period. Furthermore, the air traffic controller occasionally refuses the request for a CDO and cancels the approved CDO. The reason is that the CDO is relatively unpredictable in terms of trajectory and arrival time of the aircraft for air traffic controllers as compared to conventional operations. Accordingly, for improving the predictability of the CDO, promoting its implementation is necessary.

To this effect, various studies have previously been conducted on the prediction of the CDO. One of the most successful studies is on the Trajectory Synthesizer (TS) developed in the 1980s (Lee and Erzberger 1983, Erzberger and Chapel 1985). The TS is integrated into the Traffic Management Advisor (TMA), a decision support tool for en route air traffic controllers to calculate the estimated arrival time of an aircraft (Nedell et al. 1990). The TS is continually improved and incorporated into the Efficient Descent Advisor (EDA) (Xue and Erzberger 2010). de Jong et al. (2015) develops the aircraft-based systems called Time and Energy Managed Operations (TEMO) by combining the strategic and tactical trajectory replanning algorithm. Although TEMO is an aircraft-based on-board system, the trajectory prediction method used as the strategic algorithm can be applied to the ground-based system. Stell (2010) insists that knowing the vertical path is important for resolving conflict and focusing on the location of top of descent (TOD) for CDO. The author predicts the TOD location by combining model- and data-based techniques. In Japan, Fukushima, Hirabayashi, and Oka (2014) investigated the potential applicable time of the CDO at the KIX. They analyzed the dayplan data, which contains submitted flight plans by airlines, and it shows the

feasibility of the CDO during daytime. However, the analysis is strategic and does not include trajectory prediction based on the aircraft model.

The trajectory predictor for the CDO is widely studied particularly by a series of studies on TS. However, most trajectory predictors focus on descending from cruise to metering fix (10,000 ft). One of the problems faced in implementing CDO at the KIX is crossing arrival and departure routes near the airport. As a reason, the air traffic controllers require trajectory prediction also to be below 10,000 ft. This paper introduces the design methodology of a fast-time simulator (FTS) for simulating CDO at the KIX. The FTS means a numerical simulator based on differential equations as against a full flight simulator (FFS) which is a real-time simulator with full avionics mainly for pilot training. The FTS can simulate the predicted trajectory, arrival time, and fuel consumption of the CDO. The trajectory is calculated by simulating the flight management system (FMS) based on the dynamical model and performance model of the aircraft. The FFS experiment is also conducted to derive the reference data of the CDO.

This paper is organized as follows. Section 2 shows the FFS experiment results. The CDO routes at the KIX are explained, and the simulation conditions are set to simulate the CDO to the KIX. The simulation result is compared with the result of using the conventional descent procedure to show fuel reduction when applying the CDO. Section 3 describes the calculation flow of the FTS for simulating the CDO. This section also explains the dynamical and performance model of the aircraft. Section 4 shows the preliminary result of the FTS. The accuracy of the FTS is reviewed by comparing with the result of the FFS. Discussions are provided to show the source of the prediction error from the point of view of the actual operational environment. Section 5 concludes and summarizes our future work.

2 FULL FLIGHT SIMULATOR EXPERIMENT

2.1 Simulation Conditions

KIX has 4 CDO routes to Runway 24 called RWY24 CDO Number 1 to 4 (Ministry of Land, Infrastructure, Transport and Tourism 2017). This study focuses on RWY24 CDO Number 1, because it has the most traffic from among the four runways. Boeing 737–800 FFS is used to simulate the CDO. Figure 1 shows the simulation route. In this simulation, the aircraft flies from MIDAI and descends with a CDO at the KIX. The red line denotes the route of RWY24 CDO Number 1. The aircraft follows the route without vectoring. After passing the initial approach fix (IAF), the aircraft enters the approach phase and flies on the basis of the instrument approach chart. The prediction error of the trajectory is relatively small in the approach phase. Accordingly, the IAF (MAYAH) is set as the terminal position in the simulation. The simulation results are evaluated in the range of 250 NM from MAYAH.

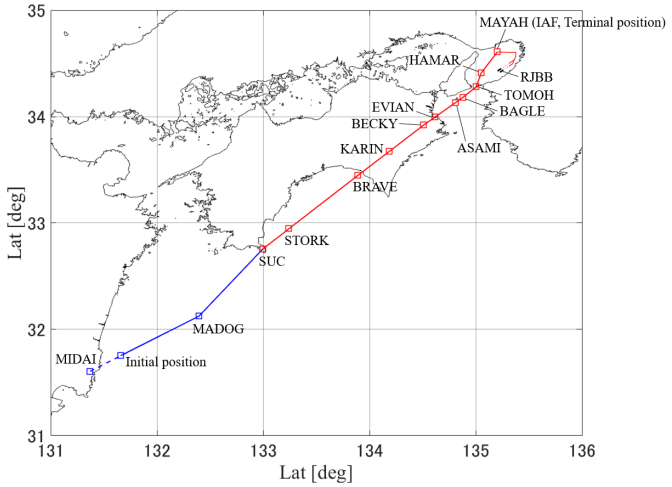

Figure 1: Simulation route.

Tables 1 and 2 show the simulation conditions. Subscripts $_0$ and $_f$ denote the initial and terminal values, respectively. Cost index (CI) is set as the typical value for the airline operations. The cruise mach number M_0 is decided by the FMS based on the CI and wind information. The Vertical Navigation Path (VNAV PTH) mode is used for descent without altitude constraints until MAYAH. The atmospheric model is set as International Standard Atmosphere (ISA). The wind conditions are interpolated linearly between 0 to 29,000 ft and are set constant above 29,000 ft.

Table 1: Boundary conditions.

	Symbol	Value	Unit
Pressure altitude	Hp_0	39000	ft
	Hp_f	4000	ft
Mach number	M_0	0.79	–
Aircraft mass (at MIDAI)	m_0	122358	lbs

Table 2: Wind conditions.

Hp [ft]	Direction [deg]	Speed [kt]
29000	320	20
0	197	13

The conventional descent procedure is also simulated to review the benefits of the CDO. In the conventional case, the aircraft descends by following the air traffic control instructions.

2.2 Simulation Results

Figure 2 shows the simulation results. The figure on the left shows the vertical path (Hp vs. distance to go to MAYAH $Dist_{togo}$). The others show the time history of the ground-related flight path angle (FPA) γ_{GS} and the fuel flow FF. The horizontal axis shows the time required to go to MAYAH t_{togo}. The blue and red lines show the results of using the CDO and conventional procedure, respectively. The red dotted and chain lines show waypoints STORK and KARIN, respectively,

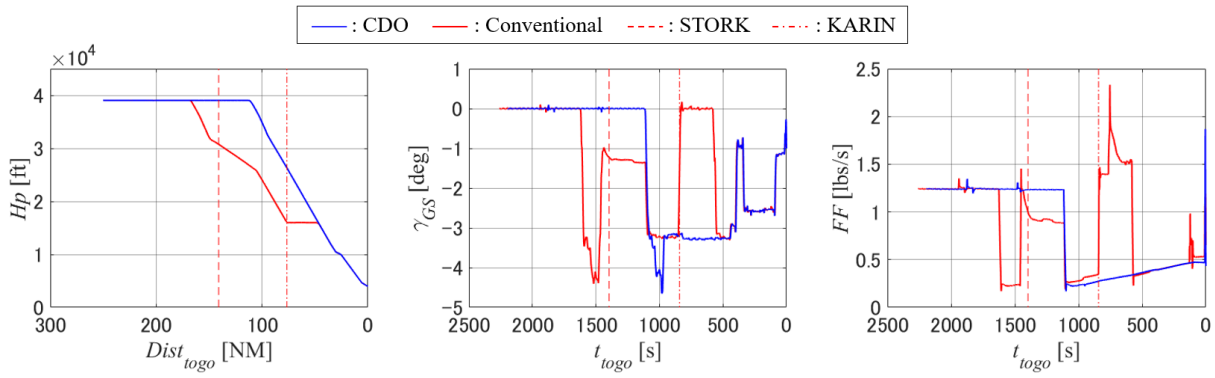

Figure 2: Simulation results of full flight simulator experiments.

In the CDO, the descent is continuous, without level segments. However, in the conventional case, the descent starts earlier than in the CDO, and the level flight begins from KARIN. The time history of γ_{GS} also shows an earlier descent and level flight. There are sector boundaries at STORK and KARIN (Ministry of Land, Infrastructure, Transport and Tourism 2017). In the conventional case, the aircraft is maintained at 29,000 ft at STORK and at 16,000 ft at KARIN when the air traffic controllers hand over the aircraft

between sectors. The aircraft starts to descend earlier than in the CDO to meet the restriction at STORK. The air traffic controller hands over the aircraft just before crossing STORK, and the restriction is canceled after the handover in this case. The aircraft continues to descend with relatively shallower FPA and then in a steeper manner to satisfy the restriction at KARIN. After KARIN, the aircraft cruises at 16000 ft until it meets the FMS-calculated optimal descent path. The figure on the right shows that the FF increases with a shallower descent and level flight, while the CDO maintains minimum FF during descent.

Table 3 shows the flight time and fuel consumption of the FFS experiments. The results show that the CDO can reduce fuel consumption to 171.77 lbs. The efficiency of the CDO is confirmed by the FFS experiments. The results of the FFS are used as reference data for the developed FTS.

Table 3: Flight time and fuel consumption of FFS experiments.

	Flight time [s]	Fuel consumption [lbs]
CDO	2195.10	1745.76
Conventional	2259.22	1917.53

3 FAST-TIME SIMULATOR FOR CDO

3.1 Calculation Flow

The FTS is developed to simulate the CDO. Figure 3 shows the typical trajectory of the CDO at the KIX. The figure on the left shows the vertical path, and that on the right shows the time history of the calibrated air speed V_{CAS} and mach M. The aircraft cruises with cruise mach M_{crz} in the cruise phase. At the TOD, the aircraft starts to descend with M_{crz}. The speed control is switched from mach-based to CAS-based on reaching crossover altitude Hp_{trans}, and the aircraft descends with descent CAS $V_{CAS,des1}$. The M_{crz} and $V_{CAS,des1}$ are calculated by the FMS based on the input CI. Civil Aeronautics Act stipulates that V_{CAS} must not exceed 250 kt below 10,000 ft in Japanese airspace. The speed restriction for the FMS is generally set as 240 kt below 10,000 ft so as to not exceed the speed limit. The aircraft rapidly decelerates to obey the restriction just before reaching 10,000 ft. The aircraft continues to descend to the IAF and decelerate again just before the IAF. In the VNAV PTH mode, M_{crz}, $V_{CAS,des1}$, and $V_{CAS,des2}$ are used to just plan the descent path, and the aircraft does not always maintain these speeds. However, the FTS assumes that the aircraft maintains the speed as M_{crz}, $V_{CAS,des1}$, and $V_{CAS,des2}$, as shown in Figure 3 to facilitate to simulate the FMS-calculated speed.

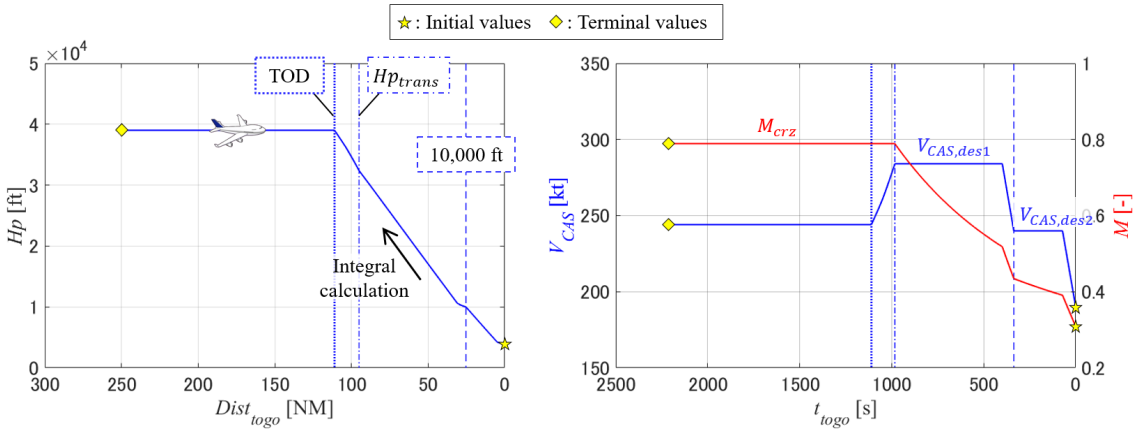

Figure 3: Typical vertical path and speed of CDO.

The CDO trajectory is calculated through an integration using the fourth order Runge-Kutta method. In the integration, the trajectory is calculated in the reverse direction. The initial value for the integration

is set as the IAF (MAYAH), which is the terminal position in the FFS experiment, and the terminal value is set as the initial position in the FFS experiment.

Figure 4 shows the flowchart of the FTS. The speed profile generation provides the profile of V_{CAS} and M by simulating the FMS. The FTS uses the ISA as an atmospheric model. The atmospheric properties are calculated according to the ISA. V_{CAS} and M are converted to true air speed V_{TAS} and ground speed V_{GS} with the atmospheric properties and wind data. The flight dynamics calculation determines the fuel consumption and motion of the aircraft by integration. The details of each component are explained in the following sections. The calculation is terminated when $Dist_{togo}$ reaches $Dist_{togof}$. $Dist_{togof}$ is set as 250 NM to simulate the CDO, as shown in 2.2.

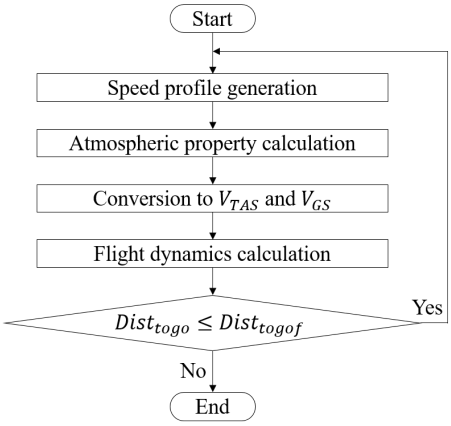

Figure 4: Flowchart of FTS.

3.2 Speed Profile Generation

The FTS calculates the trajectory in the reverse direction. At first, the speed profile generation increases V_{CAS} from the initial value to $V_{CAS,des2}$ linearly. V_{CAS} is maintained as $V_{CAS,des2}$ after reaching $V_{CAS,des2}$. When the aircraft reaches 10,000 ft, V_{CAS} is increased again up to $V_{CAS,des1}$ linearly. The speed profile generation maintains V_{CAS} as $V_{CAS,des1}$ by the time the aircraft reaches transition altitude Hp_{trans}, also called the crossover altitude. Hp_{trans} is derived by

$$Hp_{trans} = \frac{1000T_0}{0.3048 \cdot 6.5} \left(1 - \left(\frac{\left(1 + \left(\frac{\kappa-1}{2}\right)\left(\frac{V_{CAS,des1}}{a_0}\right)^2\right)^{\left(\frac{\kappa}{\kappa-1}\right)} - 1}{\left(1 + \frac{\kappa-1}{2}M_{crz}^2\right)^{\left(\frac{\kappa}{\kappa-1}\right)} - 1} \right)^{\left(-\frac{\beta_{T,<}R}{g_0}\right)} \right).$$

T_0 is the standard atmospheric temperature at Mean Sea Level (MSL), κ is the adiabatic index of air, a_0 is the speed of sound, $\beta_{T,<}$ is the ISA temperature gradient with altitude below the tropopause, R is the real gas constant for air, and g_0 is the gravitational acceleration. After crossing Hp_{trans}, the speed profile is switched from CAS-based to mach-based. M is maintained as M_{crz} until the aircraft reaches $Dist_{togof}$.

3.3 Atmospheric Property Calculation

In this section, we calculate atmospheric properties according to the ISA. Temperature T is given as

$$\begin{cases} T_< = T_0 + \beta_{T,<} Hp & (Hp < Hp_{trop}) \\ T_\geq = T_0 + \beta_{T,<} Hp_{trop} & (Hp_{trop} \leq Hp), \end{cases}$$

where subscripts $_<$ and $_\geq$ denote below and above the tropopause, respectively. Accordingly, $T_<$ denotes the temperature below the tropopause, and $T_\geq$ denotes the temperature above the tropopause. Hp_{trop} denotes the tropopause altitude, which is defined as 11,000 ft. Atmospheric pressure p is given as

$$\begin{cases} p_< = p_0 \left(\dfrac{T_<}{T_0} \right)^{-\frac{g_0}{\beta_{T,<} R}} & (Hp < Hp_{trop}) \\ p_\geq = p_0 \left(\dfrac{T_{trop}}{T_0} \right)^{-\frac{g_0}{\beta_{T,<} R}} \exp\left(-\dfrac{g_0}{R T_\geq} \left(Hp - Hp_{trop} \right) \right) & (Hp_{trop} \leq Hp). \end{cases}$$

p_0 is the standard atmospheric pressure at MSL, and T_{trop} is the temperature at the tropopause. Air density ρ is obtained by

$$\rho = \frac{p}{RT}.$$

3.4 Conversion to TAS and GS

V_{CAS} and M derived in the speed profile generation are converted to V_{TAS} as

$$\begin{cases} V_{TAS} = \left(\dfrac{2p}{\rho} \dfrac{\kappa}{\kappa - 1} \left(\left(1 + \dfrac{p_0}{p} \left(\left(1 + \dfrac{\rho_0}{2p_0} \dfrac{\kappa - 1}{\kappa} V_{CAS}^2 \right)^{\frac{\kappa}{\kappa - 1}} - 1 \right) \right)^{\frac{\kappa - 1}{\kappa}} - 1 \right) \right)^{\frac{1}{2}} & (Hp < Hp_{trans}) \\ V_{TAS} = M \sqrt{\kappa R T} & (Hp_{trans} \leq Hp). \end{cases}$$

V_{TAS} is converted to V_{GS} as

$$V_{GS} = V_{TAS} \cos \gamma_{TAS} - V_w \cos \left(\psi_{AC} - \psi_w \right),$$

where it is assumed that the draft angle is small and can be ignored. γ_{TAS} is the airmass-related FPA, V_w is the wind velocity, ψ_{AC} is the heading angle of the aircraft, and ψ_w is the wind direction.

3.5 Flight Dynamics Calculation

The flight dynamics calculation determines the fuel consumption and position by integration. The aircraft is modeled as a point mass to calculate the flight dynamics. Base of Aircraft Data (BADA) 3 developed by EUROCONTROL is used as the performance model of the aircraft (EUROCONTROL Experimental Centre 2013).

TAS acceleration acc_{TAS} is derived by time derivative of V_{TAS} as

$$acc_{TAS\,i} = \frac{V_{TAS\,i} - V_{TAS\,i-1}}{t_{togo\,i} - t_{togo\,i-1}},$$

where i denotes the number of the calculation step. Lift coefficient C_L is given as

$$C_L = \frac{2 m g_0}{\rho V_{TAS}^2 S},$$

where m is the aircraft mass, and S is the reference wing surface area. Drag coefficient C_D is defined as

$$C_D = C_{D0} + C_{D2} C_L^2.$$

C_{D0} and C_{D2} denote the parasitic and induced drag coefficients provided by BADA 3. Aerodynamic drag D is defined as

$$D = \frac{C_D \rho V_{TAS}^2 S}{2}.$$

Descent thrust Thr_{des} is formulated as

$$Thr_{des} = C_{Tdes} C_{Tc1} \left(1 - \frac{H_p}{C_{Tc2}} + C_{Tc3} H_p^2\right).$$

C_{Tdes} is the descent thrust coefficient, and C_{Tc1} to C_{Tc3} are the climb thrust coefficients provided by BADA 3. Owing to the equilibrium of force, the thrust in cruise phase Thr_{cr} is given as

$$Thr_{cr} = D.$$

By the equilibrium equation of forces, γ_{TAS} in the descent phase is derived as

$$\gamma_{TAS} = \sin^{-1}\left(\frac{-macc_{TAS} + Thr - D}{mg_0}\right).$$

As a function of Thr and V_{TAS}, fuel flow FF has the form

$$FF = C_{f1}\left(1 + \frac{V_{TAS}}{C_{f2}}\right) Thr.$$

C_{f1} and C_{f2} are the thrust specific fuel consumption coefficients provided by BADA 3. FF in the cruise phase is corrected with cruise fuel flow correction coefficient C_{fcr} as

$$FF_{cr} = C_{fcr} FF.$$

The position and m are calculated by integrating the differential equations as follows:

$$\frac{d}{dt}\begin{pmatrix} Dist_{togo} \\ Hp \\ m \end{pmatrix} = \begin{pmatrix} V_{GS} \\ V_{TAS} \sin\gamma_{TAS} \\ -FF \end{pmatrix}.$$

The total fuel consumption can be derived by subtracting m_0 from m_f.

3.6 Lift Correction Coefficient

The flight dynamics model is defined in the previous section; however, this model contains an error owing to the model approximation. Figure 5 shows the results of the FFS experiments; see 2.2.

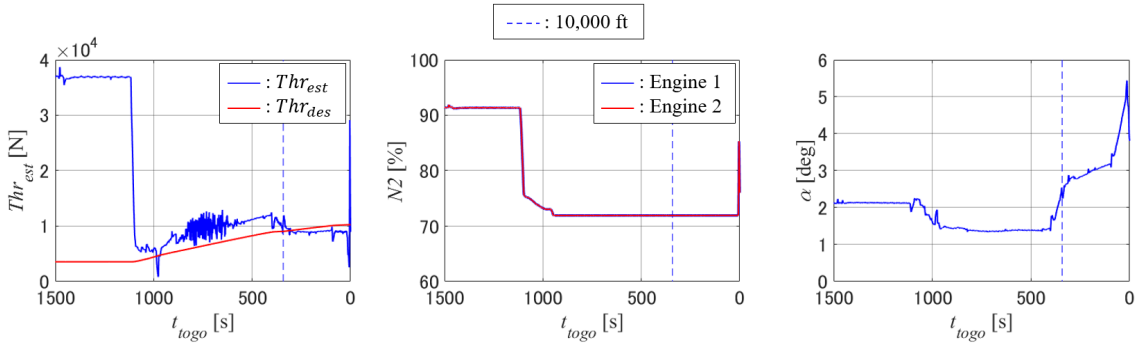

Figure 5: Simulation results of FFS experiments.

Each figure shows the time history of Thr, $N2$, and angle of attack α. Actual thrust is unavailable in the FFS experiments. Estimated thrust Thr_{est} is derived using the equilibrium equation of forces in the point mass model as

$$Thr_{est} = macc_{TAS} + D + mg_0 \sin\gamma_{TAS},$$

where D is also estimated using BADA 3. Generally, the thrust in descent increases smoothly as Thr_{des}. However, Thr_{est} steps down nonlinearly around 10,000 ft. The time history of $N2$ shows that the aircraft maintains constant thrust, which is considered idle thrust. This result indicates that the flight dynamics model contains an error owing to the definition of point mass approximation. The effects of α are assumed to be relatively large because C_L, which is used to estimate D, is proportional as α in the range of the nominal operation (Hull 2007). To correct the modeling error, C_L correction coefficient C_{C_L} is introduced as follows:

$$C_L = C_{C_L}\frac{2mg_0}{\rho V_{TAS}^2 S} \qquad \begin{cases} C_{C_L} = C_{C_L 1} & (10000 \le Hp) \\ C_{C_L} = C_{C_L 2} & (Hp < 10000). \end{cases}$$

C_L is proportional to α. The best way to introduce the correction factor is to set C_{C_L} as the function of α. However, α cannot be derived in the flight. C_{C_L} is defined as a constant value to simplify the calculation.

4 ACCURACY OF FAST-TIME SIMULATOR

4.1 Simulation Example

The simulation is conducted to review the FTS. The results of the FFS are used as reference data. The boundary conditions and wind conditions are set as in FFS. The integral time step is set as 0.01 s.

Figure 6 and Table 4 show the simulation results of the FTS. The upper left figure shows the vertical path. The other figures show the time history of M, V_{CAS}, V_{TAS}, V_{GS}, γ_{GS}, and FF.The blue and red lines show the results of FFS and FTS, respectively. The dotted and chain lines denote Hp_{trans} and 10,000 ft, respectively.

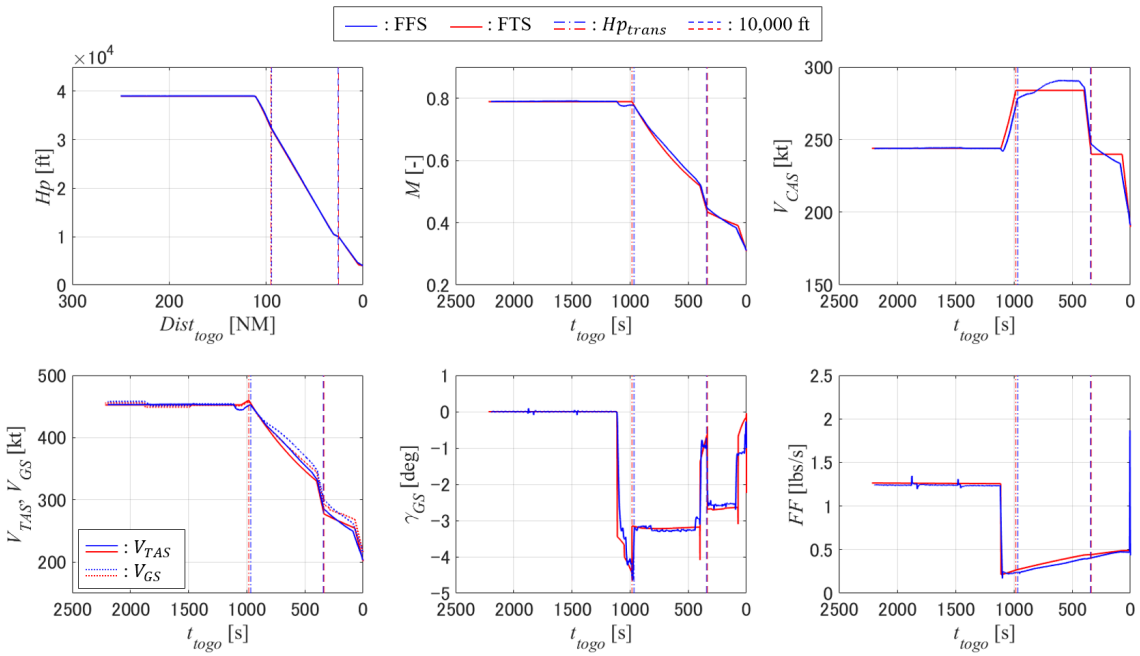

Figure 6: Simulation results of FTS.

Table 4: Simulation results.

	Flight time [s]	Fuel consumption [lbs]
FFS	2195.10	1745.76
FTS	2216.80	1818.64
Error	21.70 (1 [%])	72.88 (4 [%])

Regarding the flight time, Xue and Erzberger (2011) say that the accuracy requirement for the trajectory predictor is within 30 s at the metering fix. Harada et al. (2013) shows that the accuracy of BADA regarding the fuel consumption is within $\pm 5\%$. It seems that the FTS is accurate enough to predict the CDO by consulting these preceding studies. However, the simulation is conducted with just one case. The simulation conditions are derived from the FFS experiment results without any error. It is not sufficient to evaluate the accuracy of the FTS. The FTS has to be reviewed with various simulation conditions, such as aircraft type, cruise altitude, and cruise speed and wind conditions, using actual operational data of the CDO. Particularly as the trajectory predictor for air traffic controllers, the effects of the simulation condition errors must be investigated. The distribution of the simulation condition error can be obtained by the statistical analysis of the actual data. With several adjustments being taken into account such a distribution, the FTS can predict the CDO trajectory as shown the simulation results even in the actual operation environment.

The framework of the FTS is designed, and the simulation presents that it is useful in predicting the CDO. The next section provides the discussions regarding the error source for the FTS considering a practical operational environment.

4.2 Discussion

The FTS is developed as a ground-based trajectory predictor for air traffic controllers. The calculated trajectories can help air traffic controllers with checking separation between aircraft. Novel communication and surveillance systems are developed and implemented such as Automatic Dependent Surveillance-Broadcast (ADS-B) and Downlink Aircraft Parameters (DAPs). However, this study assumes that the FTS can only use the data via current radar data systems such as Air Route Surveillance Radar (ARSR). Table 5 shows the data list that the FTS requires to calculate the CDO and availability of the data on ground systems. "Y" denotes that the ground systems can derive the data directly. "N" denotes that the data is unavailable on the ground systems. ARSR provides the aircraft ID, latitude, longitude, and pressure altitude. The data processing system provides the aircraft type and route to air traffic controllers by referring to the submitted flight plan. Hp_f is not available on ground systems, but the terminal altitude at the IAF is restricted at 4000 ft. The aircraft can meet Hp_f accurately, and the FTS can predict that Hp_f is 4000 ft.

Table 5: Input data list for FTS and availability of data.

FTS	Aircraft type	Route	Hp_0	Hp_f	Wind data	m_f	Speed profile	C_{C_L}
Ground	Y	Y	Y	N	Y	N	N	N

The FTS can obtain the wind data from the Numerical Weather Prediction (NWP) provided by the Japan Meteorological Agency (Japan Meteorological Agency 2017). The accuracy of the wind data is within 5 m/s (Totoki et al. 2013). The effect of the wind prediction error is limited, but the sensitivity of the FTS against the wind prediction error should be investigated to predict accurately the CDO for traffic controllers. Several studies have previously been conducted to analyze the effect of the wind prediction error in the numerical simulation (Andreeva-Mori and Uemura 2016). The current ground system cannot obtain the aircraft mass, speed profile, and C_{C_L}. One solution to estimate these parameters is to analyze the actual flight data such as Quick Accuses Recorder (QAR) data of the CDO statistically. Xue and Erzberger (2011) proposes the data correction method for these parameters by using actual flight data provided by airlines. In the actual operational environment, the wind prediction error, aircraft mass, speed profile, and

C_{C_L} can become major error sources for the FTS. However, the error can be reduced by analyzing the actual flight data and tuning the FTS with the estimated parameters.

5 CONCLUSIONS AND FUTURE PLANS

This paper investigates the design methodology of the FTS to predict the CDO at the KIX. The FFS experiment is conducted to show the efficiency of the CDO and review the FTS. The experimental results show that the fuel consumption of the CDO is less than that of the conventional descent operation. The calculation method of the FTS is developed to simulate the FMS-calculated descent profile of the CDO. The FTS calculates the trajectory of the aircraft following the simulated CDO profile and provides the flight time and fuel consumption. The error source owing to point mass approximation is explained with showing the time history of the angle of attack of the FFS experiment. C_L correction coefficient is introduced to compensate the error. The simulation result shows that the FTS has sufficient accuracy to predict the CDO with accurate simulation conditions. However, it is supposed that the FTS contains an error because of the several error sources in the actual operation. The error source for the FTS is discussed to investigate the expected error in the actual operation. Considering the data availability of the ground systems, it is presumed that the major error sources are the wind prediction accuracy, aircraft mass, speed profile, and C_L correction coefficient.

Future work includes proposing a solution for reducing the error. The wind prediction error is obtained by analyzing the NWP data. The QAR data is used to estimate the typical value of the aircraft mass, speed profile, and C_L correction coefficient for the CDO flight to the KIX. The trajectory of the aircraft requesting the CDO at the KIX can definitely be predicted with high accuracy by using the FTS framework proposed in this study.

REFERENCES

Andreeva-Mori, A., and T. Uemura. 2016, Oct. "Optimal Top of Descent Analysis in Respect to Wind Prediction Errors and Guidance Strategies". In *Proceedings of the 2016 Asia-Pacific International Symposium on Aerospace Technology (APISAT)*. Toyama.

Clarke, J.-P. B., N. T. Ho, L. Ren, J. A. Brown, K. R. Elmer, K.-O. Tong, and J. K. Wat. 2004. "Continuous Descent Approach: Design and Flight Test for Louisville International Airport". *Journal of Aircraft* 41 (5): 1054–1066.

de Jong, P. M. A., N. de Gelder, R. P. M. Verhoeven, F. J. L. Bussink, R. Kohrs, M. M. van Paassen, and M. Mulder. 2015. "Time and Energy Management During Descent and Approach: Batch Simulation Study". *Journal of Aircraft* 52 (1): 190–203.

Erzberger, H., and J. Chapel. 1985, Aug. "Ground Based Concept for Time Control of Aircraft Entering the Terminal Area". In *Proceedings of the AIAA Guidance, Navigation and Control Conference*, Number 85-1888. Snowmass, Colorado.

EUROCONTROL Experimental Centre 2013, May. *User Manual for the Base of Aircraft Data (BADA) Revision 3.11*. EUROCONTROL Experimental Centre. EEC Technical/Scientific Report No. 13/04/16-01.

Fukushima, S., H. Hirabayashi, and M. Oka. 2014, Apr. "Study on Continuous Descent Operation Possibility in the En Route Airspace". In *Proceedings of the 45th JSASS Annual Meeting*. Tokyo.

Harada, A., Y. Miyamoto, Y. Miyazawa, and K. Funabiki. 2013. "Accuracy Evaluation of an Aircraft Performance Model with Airliner Flight Data". *Transactions of the Japan Society for Aeronautical and Space Sciences, Aerospace Technology Japan* 11:79–85.

Hull, D. G. 2007. *Fundamentals of Airplane Flight Mechanics*. 1st ed. Berlin, Heidelberg: Springer-Verlag.

Japan Meteorological Agency 2017. "Numerical Weather Prediction Activities". http://www.jma.go.jp/jma/en/Activities/nwp.html. Accessed data: 13 May 2017.

Kansai Airports 2016, Sep. "Kansai International Airport Smart Island Report 2016". http://www.kansai-airports.co.jp/en/efforts/environment/kix/smart-island/file/smart_rprt16.pdf.

Lee, H. Q., and H. Erzberger. 1983, Aug. "Time Controlled Descent Guidance Algorithm for Simulation of Advanced ATC Systems". Technical report, NASA. Technical Memorandum 84373.

Ministry of Land, Infrastructure, Transport and Tourism 2017. "eAIP Japan". https://aisjapan.mlit.go.jp/Login.do. Publication data: 27 Apr 2017.

Nedell, W., H. Erzberger, and F. Neuman. 1990, May. "The Traffic Management Advisor". In *Proceedings of the American Control Conference*, 514–520. San Diego, California.

Stell, L. L. 2010, Sep. "Predictability of Top of Descent Location for Operational Idle-thrust Descents". In *Proceedings of the 10th AIAA Aviation Technology , Integration, and Operations (ATIO) Conference*, Number AIAA 2010-9116. Fort Worth, Texas.

Totoki, H., T. Kozuka, Y. Miyazawa, and K. Funabiki. 2013. "Comparison of JMA Numerical Prediction GPV Meteorological Data and Airliner Flight Data". *Aerospace Technology Japan* 12:57–63.

Xue, M., and H. Erzberger. 2010, Sep. "Development and Testing of Automation for Efficient Arrivals in Constrained Airspace". In *Proceedings of the 27th International Congress of the Aeronautical Sciences (ICAS)*, Number ICAS2010-11.11.3. Nice.

Xue, M., and H. Erzberger. 2011, Sep. "Improvement of Trajectory Synthesizer for Efficient Descent Advisor". In *Proceedings of the 11th AIAA Aviation Technology, Integration, and Operations (ATIO) Conference*, Number AIAA 2011-7020. Virginia Beach, Virginia.

AUTHOR BIOGRAPHIES

DAICHI TORATANI is a researcher at the Air Traffic Management Department of Electronic Navigation Research Institute (ENRI), Japan. He holds a Ph.D. in Environment and System Sciences from Yokohama National University, Kanagawa Japan. His research interests include optimization, control, simulation and its applications in air traffic management, and unmanned aircraft systems. His e-mail address is toratani-d@mpat.go.jp.

NAVINDA KITHMAL WICKRAMASINGHE is a researcher at the Air Traffic Management Department of Electronic Navigation Research Institute (ENRI) Japan. He holds a Ph.D. in Aeronautics and Astronautics from Kyushu University, Fukuoka, Japan. His research interests include aircraft performance modeling, aircraft noise abatement, and optimal control applications in 4D-trajectory based operations. His e-mail address is navinda@mpat.go.jp.

SACHIKO FUKUSHIMA is the Deputy Director at the Air Traffic Management Department of Electronic Navigation Research Institute (ENRI) Japan. She received her Bachelor's degree in Mathematics from the University of Tsukuba, Japan in 1990. Her research focuses on the expansion of optimal profile descent operations. Her email address is sachiko@mpat.go.jp.

HIROKO HIRABAYASHI is a senior researcher at the Air Traffic Management department of Electronic Navigation Research Institute (ENRI) Japan. She received her Master's degree in Biology from Yokohama City University, Kanagawa Japan, in 1997. She worked as an air traffic controller for 15 years. Her research interests include big data analysis and fast time simulations on technical approach for safe and efficient air traffic operations. Her e-mail address is h-hirabayashi@mpat.go.jp.